Liquid Crystals
Publication details, including instructions for authors and subscription information:
http://www.informaworld.com/smpp/title~content=t713926090

Liquid crystal properties of a mesogenic polyacetylene, poly(11-[(4'-heptoxy-4-biphenylyl)carbonyloxy]-1-undecyne)

Jianxin Geng[a]; Fengxia Geng[a]; Jiku Wang[a]; Baocai Zhu[a]; Gao Li Corresponding author[a]; Enle Zhou[a]; Jacky Wing[b]; Yip Lam[b]; Ben Zhong Tang[b]
[a] State Key Laboratory of Polymer Physics and Chemistry, Changchun Institute of Applied Chemistry, Chinese Academy of Sciences, Changchun 130022, PR China [b] Department of Chemistry, Hong Kong University of Science & Technology, Kowloon, Hong Kong, China

Online publication date: 19 May 2010

To cite this Article Geng, Jianxin , Geng, Fengxia , Wang, Jiku , Zhu, Baocai , Li Corresponding author, Gao , Zhou, Enle , Wing, Jacky , Lam, Yip and Tang, Ben Zhong(2004) 'Liquid crystal properties of a mesogenic polyacetylene, poly(11-[(4'-heptoxy-4-biphenylyl)carbonyloxy]-1-undecyne)', Liquid Crystals, 31: 2, 271 — 277
To link to this Article: DOI: 10.1080/02678290410001648589
URL: http://dx.doi.org/10.1080/02678290410001648589

LIQUID CRYSTALS, VOL. 31, NO. 2, FEBRUARY 2004, 271–277

Liquid crystal properties of a mesogenic polyacetylene, poly(11-[(4′-heptoxy-4-biphenylyl)carbonyloxy]-1-undecyne)

JIANXIN GENG, FENGXIA GENG, JIKU WANG, BAOCAI ZHU, GAO LI*, ENLE ZHOU

State Key Laboratory of Polymer Physics and Chemistry, Changchun Institute of Applied Chemistry, Chinese Academy of Sciences, Changchun 130022, PR China

JACKY WING YIP LAM and BEN ZHONG TANG

Department of Chemistry, Hong Kong University of Science & Technology, Clear Water Bay, Kowloon, Hong Kong, China

(*Received 21 October 2002; in final form 25 September 2003; accepted 4 October 2003*)

The liquid crystalline properties of a mesogenic poly(1-alkyne) and the corresponding monomer were studied using transmission electron microscopy, X-ray diffraction, polarizing optical microscopy and differential scanning calorimetry. The monomer exhibits a monotropic smectic A phase and a metastable crystalline phase. The rigid polymer backbones do not prevent the mesogenic moieties from packing into smectic A and B phases in the temperature ranges 127.6–74.1°C and 74.1°C–room temperature, respectively, on cooling from the isotropic melt.

1. Introduction

Liquid crystals (LCs) and side chain liquid crystalline polymers (SCLCPs) have been widely studied in both academic and industrial laboratories. A wide range of polymers with flexible backbones, such as polymethacrylates [1, 2] and polyacrylates [3], have been synthesized. The conventional molecular architecture for SCLCPs is 'flexible backbone + spacer + mesogenic groups' [4, 5]. Researchers in the area have paid little attention to SCLCPs with conjugated stiff backbones.

Polyacetylene, polypyrrole and polythiophene are typical organic conjugated polymers. The attachment of mesogenic moieties to a conjugated backbone is of great interest because the resulting polymers possess unique electrical, optical and LC properties [6–14]. Under external fields, these novel SCLCPs show properties different from those of conventional, flexible SCLCPs. The alignment of the polymer backbone accompanying the side chain orientation induced by a magnetic field can, for example, improve the conductivity and give rise to electrical or optical anisotropy [15–18]. Shearing can yield new textures, arising from the long relaxation time of the rigid polyacetylene backbone [19].

*Author for correspondence; e-mail: ydh@ns.ciac.jl.cn

In recent years, a number of side chain LC polyacetylenes have been synthesized [20–24], but a detailed study of their phase structures is lacking. In this work, we systematically studied the LC properties of a novel side chain liquid crystalline polyacetylene, poly (11-[(4′-heptoxy-4-biphenylyl)carbonyloxy]-1-undecyne) (PA9EO7), and those of the corresponding monomer (A9EO7) using polarizing optical microscopy (POM), differential scanning calorimetry (DSC), X-ray diffraction (XRD) and transmission electron microscopy (TEM).

2. Experimental

2.1. *Specimen preparation*

The molecular structures of A9EO7 and PA9EO7 are:

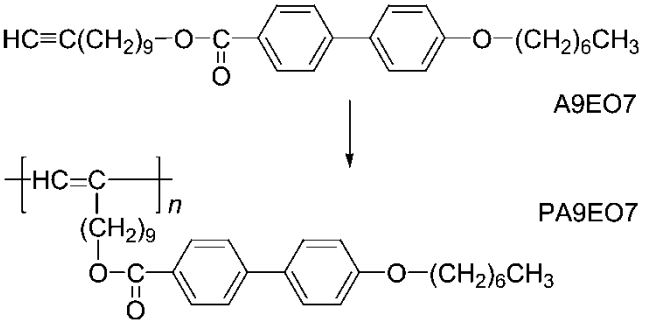

Liquid Crystals ISSN 0267-8292 print/ISSN 1366-5855 online © 2004 Taylor & Francis Ltd
http://www.tandf.co.uk/journals
DOI: 10.1080/02678290410001648589

Their synthesis and chemical properties were reported in a previous paper [25]. The number-average molecular weight of PA9EO7 is 180 000 and its stereostructure is *trans*-rich, with a *trans*-content of 85.2%. A9EO7 and PA9EO7 were dissolved in toluene to make 0.1 and 0.05 wt % solutions, respectively. The solution was dropped onto a thin carbon film precoated onto a surface of freshly cleaved mica. After the solvent evaporated, thin solid films were obtained. The PA9EO7 film was heated to the melt, cooled, and then quenched using liquid nitrogen to freeze the molecular arrangements present in the LC phase. The sample was transferred onto a Cu grid, and analysed using electron diffraction (ED); the morphology was studied by TEM.

2.2. *Instrumentation*

The DSC traces were obtained using a Parkin-Elmer DSC under nitrogen. The optical textures were observed between crossed-polarizers using an Opton POM. TEM observations and ED patterns were performed on a JEOL2010 TEM operating at 200 kV. The XRD data were measured on a Rigaku D/max 2500 PC diffractometer using CuK_α radiation with a wavelength of 1.5406 Å.

3. Results and discussion

3.1. *LC properties of A9EO7*

Figure 1 shows the DSC thermograms of A9EO7 obtained at different scanning rates. Three phase transitions at 55.7, 50.5 and 42.7°C were seen on cooling at a scanning rate of 1°C min^{-1}, as shown in figure 1 (*a*). The exothermic peaks at 55.7 and 50.5°C result from isotropic–LC and LC–crystal phase transitions, respectively. The exothermic peak at 42.7°C however is broader than those seen at 55.7 and 50.5°C, and broadens and shifts to lower temperature on increasing the scanning rate. This indicates that a much slower phase transition occurs at 42.7°C than at the other two temperatures. This exothermic peak results from a crystal (crystal II) to crystal (crystal I) phase transition, and this assignment will be discussed later. The sample was subsequently heated at the same rate as it was cooled, see figure 1 (*b*). Only a melting transition was detected at 69.5°C in the heating scan at 1°C min^{-1}, indicating the monotropic nature of the LC behaviour of A9EO7. On increasing the scanning rate, a weak endothermic peak at 57.4°C and a weak exothermic peak at 60.0°C appeared before the melting peak.

XRD experiments were performed in order to obtain information on the molecular packing arrangements within these phases. Figure 2 shows the change of the XRD patterns with temperature. Each pattern was

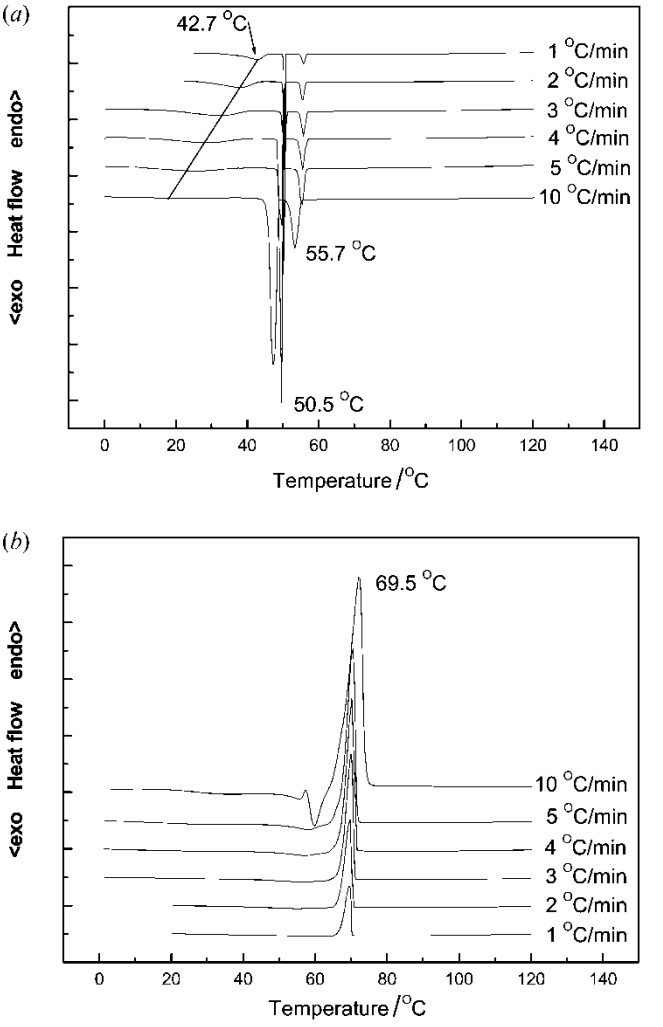

Figure 1. DSC thermograms of A9EO7 obtained at different scanning rates (*a*) cooling and (*b*) heating.

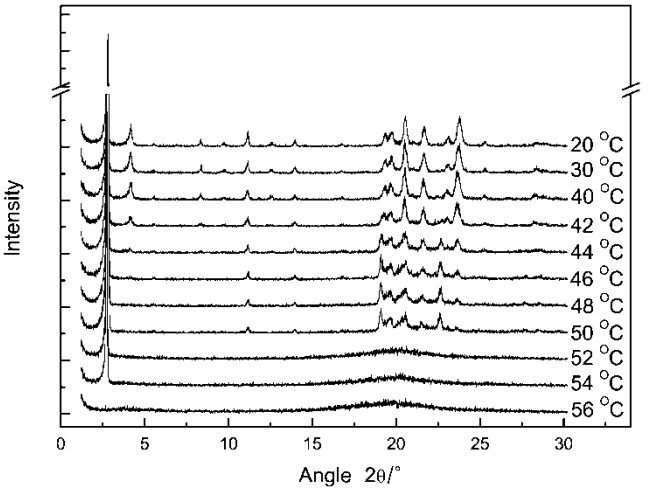

Figure 2. XRD patterns measured on cooling A9EO7 from the isotropic melt.

measured after reducing the temperature by 2°C at a cooling rate of 1°C min^{-1}. From the change in the reflection peaks in the diffractograms with temperature, the phase transition from the LC phase to crystal II takes place between 52 and 50°C. The diffractograms obtained at 54 and 52°C show a sharp reflection at low angle, $2\theta = 2.74°$, and a diffraction halo at $\sim 20°$. The reflection peak at 2.74° corresponds to a *d*-spacing of 32.22 Å, and this mesophase can be classified as a smectic A (SmA) phase.

On cooling further, the reflection peaks at 19.08 and 22.62° in the diffractograms obtained in the temperature range 50 to 44°C disappear, and four sharp reflection peaks appear at 4.17, 20.50, 21.68 and 23.97° in the diffractograms recorded below 42°C, indicating clearly a phase transition between 44 and 42°C. The phase transition temperature was measured as 42.7°C from the DSC curve, Figure 1 (*a*). We have discussed the structure of crystal I in a previous paper [26], and here focus on the crystal II phase.

To investigate further the properties of crystal II, DSC experiments were performed. The isotropic melt of A9EO7 was cooled to 49°C, i.e. the temperature at which crystal II forms, and then heated. An endothermic peak was detected at 55.7°C, which is the melting point of crystal II, see figure 3.

A structurally similar compound, 5-[(4′-heptoxy-4-biphenylyl)carbonyloxy]-1-pentyne (A3EO7) also displays a metastable mesophase [27]. The crystal II phase of A9EO7 is metastable, as indicated by the DSC experiments. A9EO7 was cooled from its isotropic melt to 49°C, and annealed at this temperature. An exothermic phenomenon was observed after ~ 40 min. When the specimen was further cooled after for annealing 90 min, the exothermic peak resulting from the crystal II to crystal I transition was observed, but the enthalpy associated with this phase transition was much smaller than for the non-annealed sample. This suggests the occurrence of crystal II to crystal I transition during the annealing process. In a reference experiment, the specimen was heated after annealing at 49°C for 90 min. As shown in figure 4, two endothermic peaks were detected, at 55.7 and at ~ 69.5°C, which correspond to the melting points of crystal II and I, respectively. In addition, an exothermic peak at 56.9°C appeared after crystal II melted. This behaviour may be interpreted as a fraction of crystal II transforming to crystal I during the annealing process. Thus, crystals II and I are in coexistence when the specimen was heated. Crystal II then melted at 55.7°C, but the existence of crystal I induce the isotropic liquid of A9EO7 to crystallize, giving the exothermic peak at 56.9°C. Crystal I melted finally on heating the specimen to 69.5°C. DSC experiments therefore show that crystal II is a metastable phase. The existence of the metastable crystal II phase also accounts for the weak endothermic peak followed by a weak exothermic peak in the heating scan at 10°C min^{-1}, figure 2 (*b*).

The optical textures of the LC phase were observed on cooling and are shown in figure 5. In the temperature range of the SmA phase, A9EO7 shows a focal-conic texture. When the specimen is cooled to crystal II the focal-conic texture becomes broken with dark lines normal to the radial direction of the former focal-conic texture. On further cooling, the lines disappear in the crystal I phase.

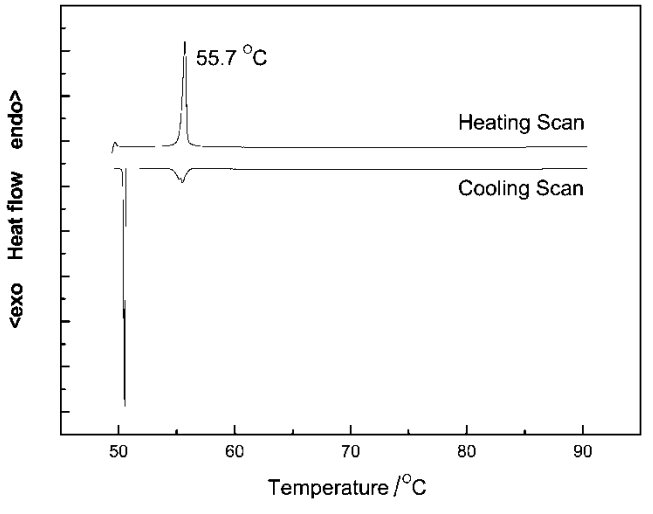

Figure 3. DSC thermogram of A9EO7 obtained at a scanning rate of 1°C min^{-1}. The specimen was cooled to crystal II from the isotropic melt, and reheated immediately.

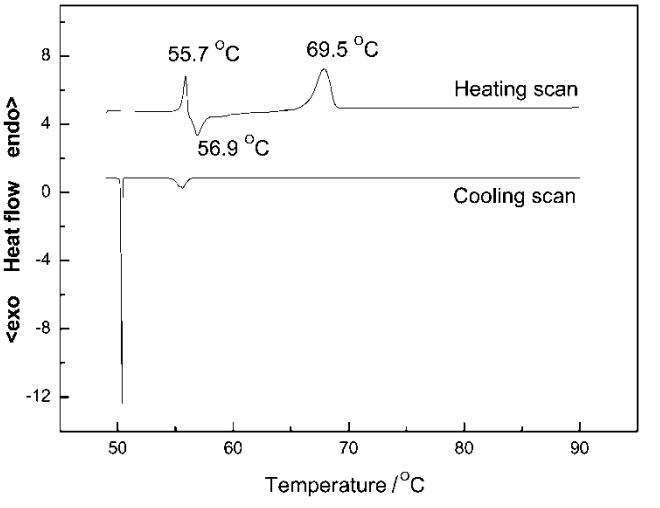

Figure 4. DSC thermograms of A9EO7 obtained at a scanning rate of 1°C min^{-1}. The specimen was cooled to crystal II, annealed for 90 min, and then heated.

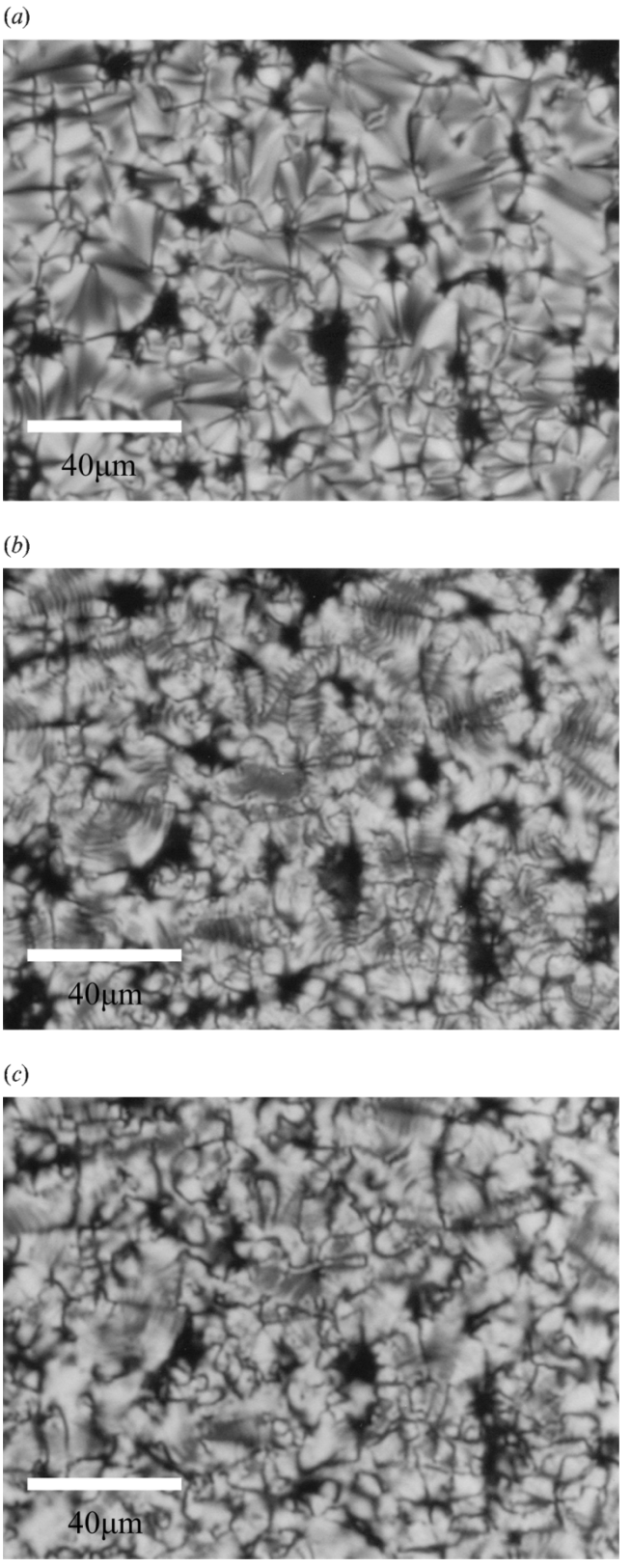

Figure 5. Optical textures of A9EO7: (*a*) focal-conic texture shown by SmA phase, (*b*) crystal II phase, (*c*) crystal I phase.

3.2. *LC properties of PA9EO7*

POM observations and DSC experiments revealed the enantiotropic LC behaviour of PA9EO7. The phase transition temperatures were determined as 127.6 and 74.1°C on cooling, 75.6, and 128.6°C on heating. To obtain structural information, XRD experiments were performed, see figure 6. The diffractogram obtained at 90°C shows two reflections at low angle, $2\theta = 2.71°$ and 5.37°, and a diffuse peak in the middle angle region of ~20°. This is characteristic of a SmA phase. The reflection peaks in the low angle give the layer periodicity, $d = 32.57$ Å, and the diffuse peak in the middle angle region gives the lateral intermolecular separation of the mesogens as $d = 4.4$ Å. The pattern shown as figure 6 (*b*) was obtained at 60°C on cooling the specimen from the SmA phase. The reflection peaks in the low angle move slightly to lower angle, thus indicating an increase in the layer periodicity ($d = 33.82$ Å). The diffraction peak at $2\theta = 20.07°$ is sharp, implying a more ordered lateral molecular packing of mesogens than in the SmA phase. Therefore PA9EO7 undergoes a transition to a smectic B (SmB) phase when cooled to 74.1°C. It is clear that the rigid biphenylyl groups are interdigitated and well packed, whereas the flexible spacers are perturbed by the rigid backbone and cannot adopt extended conformations. During the phase transition at 74.1°C, the side chains adjust their conformation to adopt as extended conformations as possible. Consequently the distance between the layer planes in the SmB phase is 1.25 Å larger than in the SmA phase.

A sample of PA9EO7 was quenched using liquid nitrogen at 110°C as described in the literature, [8, 19]. As figure 7 shows, the island-like TEM morphology

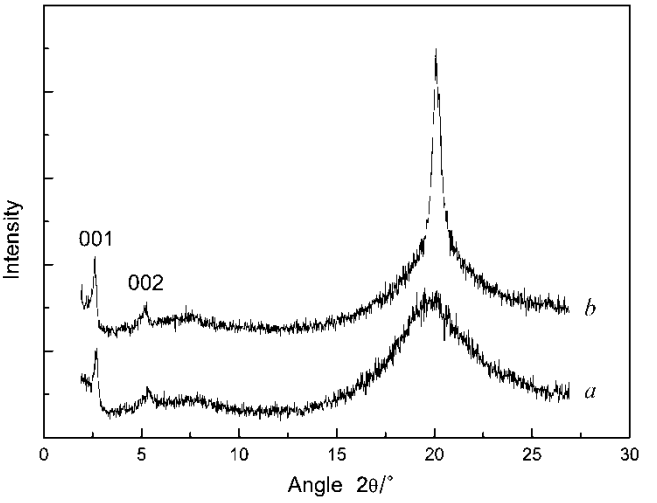

Figure 6. XRD patterns of PA9EO7 measured in the (*a*) SmA phase and (*b*) SmB phase.

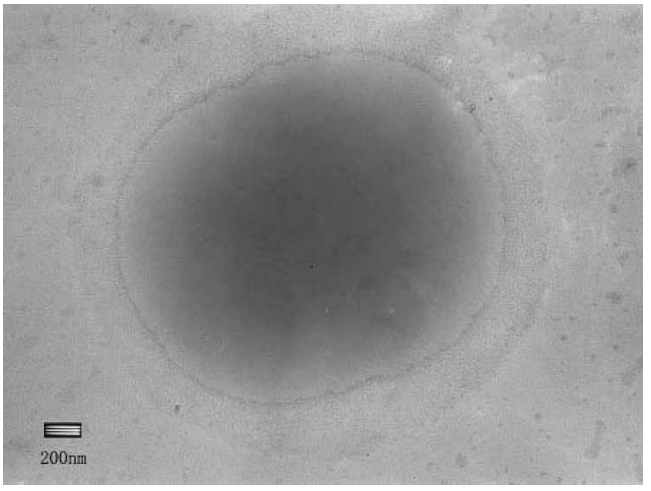

Figure 7. TEM morphology of PA9EO7 quenched using liquid nitrogen in the SmA phase.

has no regular shape. Each island is an LC domain, as its ED pattern shows the same lattice orientation. Different sample domains can give two sets of ED patterns. Figure 8 (*a*) shows a diffuse ring that corresponds to the lateral separation of the mesogens ($d = 4.4$ Å), and the electron beam is parallel to the direction of the long axes of the mesogenic moieties. In the another case, with the electron beam incident normal to the direction of the long axes of the mesogenic moieties, a different ED pattern characteristic of a smectic phase was recorded, figure 8 (*b*). The diffuse arcs on the equator correspond to the lateral separation of the mesogens. The diffraction spots on the meridian correspond to the distance between the layers of the smectic phase ($d = 32.57$ Å), and can be indexed as (0 0 *l*). Thus the ED patterns confirm the assignment of the LC phase in the temperature range 127.6–74.1°C as a SmA phase.

To enhance the molecular packing in the SmB phase, a TEM sample of PA9EO7 was annealed at 60°C for 12 h after cooling from the isotropic melt. Figure 9 shows the ED patterns of the annealed specimen. Figure 9 (*a*) gives a hexagonal two-dimensional lattice, suggesting a hexagonal close packing of mesogenic moieties. Figure 9 (*b*) is essentially the same as the ED pattern of the SmA phase, but the layer spacing obtained from the diffraction spots is larger than that in the SmA phase. These results also confirm that PA9EO7 shows a SmB phase and not a crystalline phase below 74.1°C when cooled from the isotropic melt.

There is no difference between the morphologies of the smectic B and A phases observed when the electron beam is normal to the smectic layer planes. With the electron beam parallel to the smectic layers, clear cracks

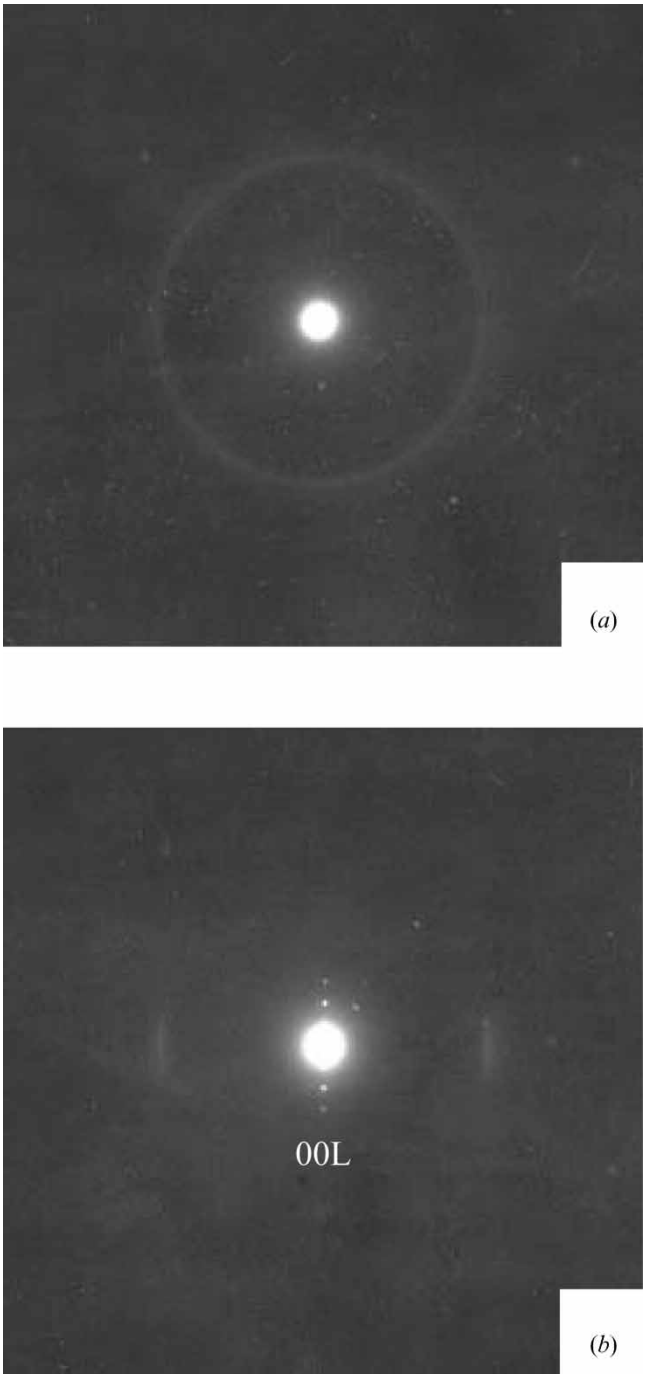

Figure 8. ED patterns of PA9EO7 in the SmA phase with electron beam incident (*a*) parallel and (*b*) normal to the long axes of the mesogenic moieties.

are seen on the surface of the morphology of the SmB phase (figure 10). This must be caused by the adjustment of the molecular conformation when PA9EO7 undergoes transition from the SmA to SmB phase and in the annealing process at 60°C. The layer planes of the SmB phase are parallel to the cracks on the surface of the domain.

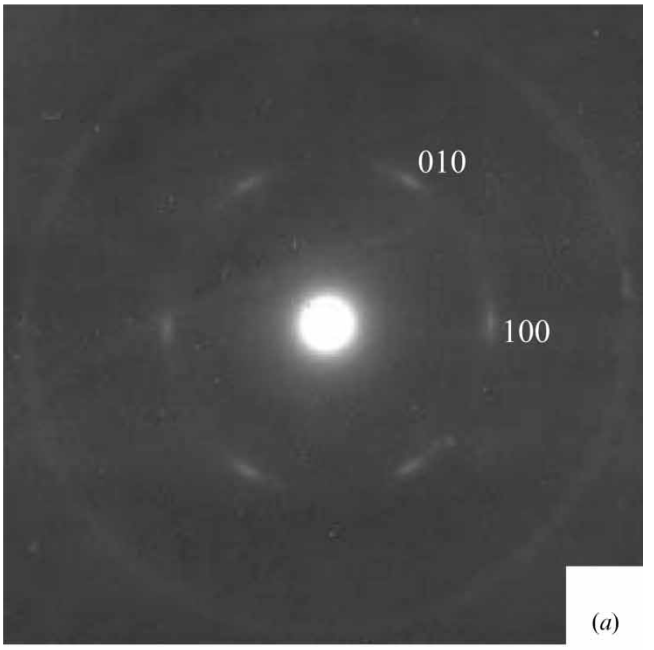

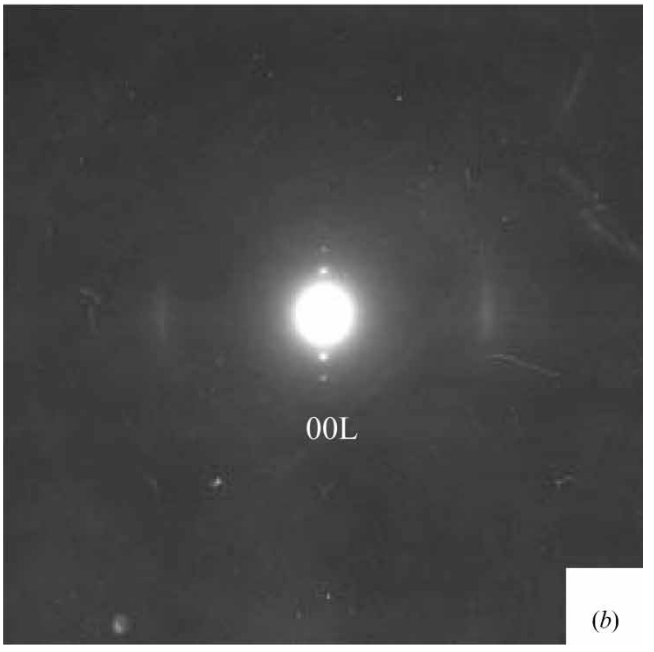

Figure 9. ED patterns of PA9EO7 in the SmB phase with the electron beam incident (*a*) parallel and (*b*) normal to the long axes of the mesogenic moieties.

4. Conclusions

In this paper, the LC properties of an acetylene monomer with a biphenyl mesogen and its polymer are described. A9EO7 displays a monotropic SmA phase, with layer spacing 32.22 Å. The crystal II is a metastable crystalline phase. The conjugated backbone of PA9EO7 is rigid. It is difficult for the polymer to rearrange into a three-dimensional lattice on cooling the isotropic melt. Consequently, PA9EO7 does not crystallize, even at room temperature. The polymer shows only SmA and SmB phases in the temperature ranges 127.6–74.1°C and 74.1°C–room temperature, respectively. Thus the rigid polymer backbone does not prevent the self-organization of the mesogenic moieties in the side chain liquid crystalline polyacetylene. This opens an avenue for the exploration of new kinds of side chain liquid crystalline polymers.

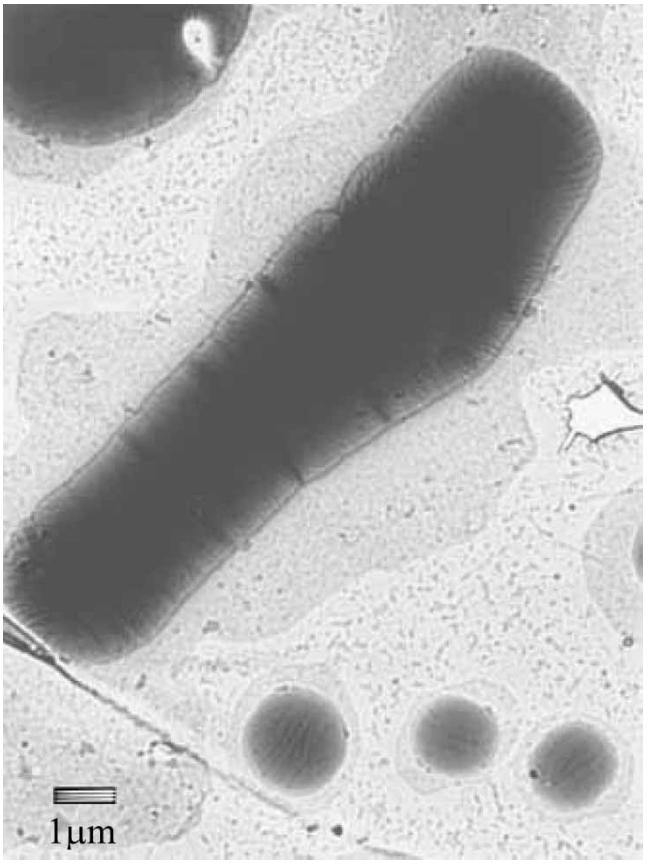

Figure 10. TEM morphology of PA9EO7 imaged with electron beam parallel to the layer planes of the smectic B phase.

We thank the National Natural Science Foundation of China (Project Nos. 29904008, 20174043 and 20023003) and the Research Grants Council of Hong Kong (Project Nos. HKUST6121/01P and 6085/02P) for financial support. This work was also supported by the Special Funds for Major State Basic Research Projects.

References

[1] HESSEL, F., and FINKELMANN, H., 1985, *Polym. Bull.*, **14,** 375.

[2] YAMAGUCHI, T., ASADA, T., HAYASHI, H., and NAKAMURA, N., 1989, *Macromolecules*, **22,** 1141.
[3] LI, M., ZHOU, E., XU, J., YANG, C., and TANG, X., 1995, *Polym. Bull.*, **35,** 65.
[4] FINKELMANN, H., RINGSDORF, H., and WENDORFF, J. H., 1978, *Makromol. Chem.*, **179,** 273.
[5] FINKELMANN, H., RINGSDORF, H., SIOL, W., and WENDORFF, J. H., 1978, *Makromol. Chem.*, **179,** 829.
[6] KANG, E. T., NEOH, K. G., MASUDA, T., HIGASHIMURA, T., and YAMAMOTO, M., 1989, *Polymer*, **30,** 1328.
[7] AKAGI, K., GOTO, H., KADOKURA, Y., SHIRAKAWA, H., OH, S.-Y., and ARAYA, K., 1995, *Synth. Met.*, **69,** 13.
[8] TANG, B. Z., KONG, X., WAN, X., PENG, H., and LAM, W. Y., 1998, *Macromolecules*, **31,** 2419.
[9] MOIGNE, J. L., and HIBERER, A., 1991, *Makromol. Chem.*, **192,** 515.
[10] HASEGAWA, H., KIJIMA, M., and SHIRAKAWA, H., 1997, *Synth. Met.*, **84,** 177.
[11] KIJIMA, M., ABE, S., and SHIRAKAWA, H., 1999, *Synth. Met.*, **101,** 61.
[12] TOYOSHIMA, R., NARITA, M., AKAGI, K., and SHIRKAWA, H., 1995, *Synth. Met.*, **69,** 289.
[13] DAI, X. M., GOTO, H., AKAGI, K., and SHIRAKAWA, H., 1999, *Synth. Met.*, **102,** 1291.
[14] DAI, X. M., NARIHIRO, H., GOTO, H., AKAGI, K., and YOKOYAMA, H., 2001, *Synth. Met.*, **119,** 397.
[15] MASUDA, K., AKAGI, K., SHIRAKAWA, H., and NISHIZAWA, T., 1998, *J. mol. Struct.*, **441,** 173.
[16] GOTO, H., and AKAGI, K., 1999, *Synth. Met.*, **102,** 1292.
[17] OSAKA, I., SHIBATA, S., TOYOSHIMA, R., AKAGI, K., and SHIRAKAWA, H., 1999, *Synth. Met.*, **102,** 1437.
[18] OSAKA, I., GOTO, H., ITOH, K., and AKAGI, K., 2001, *Synth. Met.*, **119,** 541.
[19] KONG, X., and TANG, B. Z., 1998, *Chem. Mater.*, **10,** 3352.
[20] HIN, S.-H., KIN, S.-H., CHO, H.-N., and CHOI, S.-K., 1991, *Macromolecules*, **24,** 6050.
[21] CHOI, S.-J., KIM, S.-H., AHN, W., CHO, H.-N., and CHOI, S.-K., 1994, *Macromolecules*, **27,** 4871.
[22] LINO, K., GOTO, H., AKAGI, K., SHIRAKAWA, H., and KAWAGUCHI, A., 1997, *Synth. Met.*, **84,** 967.
[23] TANG, B. Z., KONG, X., and WAN, X., 1997, *Macromolecules*, **30,** 5620.
[24] GOTO, H., AKAGI, K., and SHIRAKAWA, H., 1997, *Synth. Met.*, **84,** 373.
[25] KONG, X., LAM, W. Y., and TANG, B. Z., 1999, *Polym. Mater. Sci. Eng.*, **80,** 151.
[26] GENG, J., GENG, F., YANG, X., WANG, J., LI, G., ZHOU, E., and TANG, B., 2002, *Mol. Cryst. liq. Cryst.*, **383,** 115.
[27] GENG, J., WANG, S., LING, W., LI, G., ZHOU, E., LAM, J. W. Y., and TANG, B. *Liq. Cryst.* (to be published).